Original Article

The involvement of the laminin-integrin α7β1 signaling pathway in mechanical ventilation-induced pulmonary fibrosis

Han-Di Liao, Yong Mao, You-Guo Ying

Department of Intensive Care Unit, Shanghai 9th People's Hospital, Shanghai Jiao Tong University School of Medicine, Shanghai 201999, China

Contributions: (I) Conception and design: All authors; (II) Administrative support: None; (III) Provision of study materials or patients: None; (IV) Collection and assembly of data: All authors; (V) Data analysis and interpretation: All authors; (VI) Manuscript writing: All authors; (VII) Final approval of manuscript: All authors.

Correspondence to: Dr. You-Guo Ying. Department of Intensive Care Unit, Shanghai 9th People's Hospital, Shanghai Jiao Tong University School of Medicine, No. 280, Mohe Road, Baoshan District, Shanghai 201999, China. Email: yingyouguo@yeah.net.

Introduction: The central objective of the study was to determine the possibility and potential mechanism by which the laminin-integrin α7β1 signaling pathway acts on mechanical ventilation (MV)-induced pulmonary fibrosis in a rat model.

Methods: Fibrosis rat models were established via the mechanical injury method. Ninety rats were recruited and divided into the normal, low tidal volume (LVT), huge VT (HVT), Arg-Gly-Asp-Ser (RGDS), LVT + RGDS and HVT + RGDS groups. On day 0, 3, and 7 after model establishment, the pulmonary hydroxyproline content was measured using alkaline hydrolysis and the pulmonary index was also calculated. All rats in each group were executed on day 0, 3 and 7. The histopathological changes detected in the left pulmonary tissues were observed using hematoxylin-eosin (HE) and Masson staining methods.

Discussion: The mRNA and protein expressions of Wnt-5A, β-catenin, E-cadherin and Collagen I in the Wnt/β-catenin signaling pathway were detected using both reverse transcription quantitative polymerase chain reaction (RT-qPCR) and western blotting methods. Immunohistochemistry was employed to detect the fibronectin (FN) expression in the pulmonary tissues on the 7th day. All indexes in the RGDS and LVT + RGDS groups indicated no explicit differences compared with the normal group. In the LVT, HVT, HVT + RGDS groups, the respective weights of the rats and the expression of E-cadherin on the 7th day exhibited decreases, however the pulmonary index, hydroxyproline, pulmonary alveolar inflammation, pulmonary fibrosis, FN expression, and protein expressions of Wnt-5A, β-catenin, and Collagen I all displayed increased levels (all $P<0.05$). The index changes detected in the HVT group were the most blatant results observed in the study. The rat pulmonary index on the 7th day, hydroxyproline (HYP), pulmonary alveolar inflammation, pulmonary fibrosis, FN expression, and protein expressions of Wnt-5A, β-catenin, and type I-collagen were all down-regulated, in contrast the expression of E-cadherin was up-regulated in the LVT + RGDS and HVT + RGDS groups in comparison with the LVT and HVT groups, respectively (all $P<0.05$).

Conclusions: The findings of the study suggested that RGDS could act to block the laminin-integrin α7β1-signaling pathway, ultimately contributing to the inhibition of the progression of MV-induced pulmonary fibrosis.

Keywords: Laminin-integrin α7β1; Arg-Gly-Asp-Ser (RGDS); mechanical ventilation (MV)-induced pulmonary fibrosis; Wnt-5A; β-catenin; collagen I; E-cadherin; fibronectin (FN)

Submitted Mar 01, 2017. Accepted for publication Aug 24, 2017.
doi: 10.21037/jtd.2017.09.60
View this article at: http://dx.doi.org/10.21037/jtd.2017.09.60

Introduction

Mechanical ventilation (MV) is an indispensable clinical supportive measurement tool in many clinical scenarios including during general anesthesia or in the treatment of patients with various severe respiratory diseases (1). However, the benefits of MV run in concert with the risks associated with ventilation-induced lung injury, such as biotrauma, alveolar epithelial injury, and even the induction of pulmonary fibrosis (2). Recent studies have suggested that pulmonary fibrosis could occur in the early stage of MV and its prognosis can potentially too be affected by MV (3,4). Due to the complex pathogenesis mechanisms of pulmonary fibrosis, the triggering mechanisms of early MV-induced fibrosis still remain largely unknown (5). However, it is known that high airway pressure and large tidal volumes (VT) can lead to over distension of lung inspiration units and lung injury, which may subsequently increase the chances of fibrosis (6). Even worse, delays in either identification or treatment can result in the death of patients who suffer from severe diseases. As the medical consequences of MV-induced fibrosis has been a primary concern in the clinical world, numerous research studies continue to investigate the finer mechanism on a molecular level with an objective of providing theoretical guidance and practical experience for prevention and intervention means.

Laminins (LN) are heterotrimeric proteins that contain a α-chain, a β-chain, and a γ-chain (7). LN represents indispensable elements in lung development. LN has various roles including the induction of cell adhesion, growth and differentiation (8,9). In specific terms, LN can attract and adhere to fibroblasts, inflammatory cells, pulmonary epithelial cells and stimulate macrophages so as to facilitate epithelial cells and fibroblasts to synthesize collagen, which is the central role of laminin's complicated function in pulmonary fibrosis (10). Integrin is a trans-membrane heterodimer comprised of α and β subunits that are linked by a non-covalent bond. As the bridge between extracellular matrix and cytoskeleton, LN acts to mediate multiple cellular signal transductions, such as cell contraction, activation, secretion, proliferation, migration, differentiation and necrosis (11). Integrin α7β1 has been an LN family member studied in depth and is expressed in various cells and tissues, including skeletal muscle cells, cardiomyocyte, airway smooth muscle cells, hepatocarcinoma cells and Schwann cells (12,13). α7β1 regulates cells proliferation, migration and differentiation by binding specifically to LN through its α7 subunit (14-16). Furthermore, the activation of the Wnt/β-catenin signaling pathway is also reported to play an important role in both ventilator induced lung injury and lung repair (6). Despite its importance, it appears that no current study has investigated the possible role of the laminin-integrin α7β1 signaling pathway in MV-induced fibrosis. Therefore, this study was conducted with the aim of investigating the effects related with the molecular mechanisms involved with blocking the laminin-integrin signaling pathway in MV-induced fibrosis.

Methods

Ethics statement

All animal experiments were conducted in under strict compliance with the approved animal protocols and guidelines established by the Declaration of Helsinki. Likewise all animal experiments conducted during the study were pre-approved by the Animal ethics Association of the Shanghai 9th People's Hospital, Shanghai Jiao Tong University School of Medicine (Grant No. 201603001). All necessary efforts were made to minimize the suffering of the animals participating in the study.

Establishment of rat pulmonary fibrosis model

Ninety clean grade sprague-dawley (SD) male adult rats aged between 6–8 weeks, weighing approximately 239.62±23.57 g were recruited for the study (purchased from Model Animal Research Center of the Nanjing University, Nanjing, China). The rats were fed normally at room temperature 25±1 ℃ under humidity conditions of 55–60%. The rats underwent periods of light exposure as well as light protection each for 12 hours per day. Pads in each cage were replaced and the respective rat cages were disinfected every day. All animals underwent a period of environmental adaptation for duration of 1 week prior to the commencement of the experiment. The rats were divided into six groups (15 rats/per group): normal, low tidal volume (L_{VT}), huge VT (H_{VT}), Arg-Gly-Asp-Ser (RGDS) (blocking agent of the laminin-integrin α7β1), L_{VT} + RGDS and H_{VT} + RGDS groups. All rats were anesthetized with pentobarbital at 40 mg/kg of 3% Nembutal via intra-abdominal injection, and the trachea were incised for cannula implantation. The rats in the normal group were allowed to respire autonomously for 4 hours. In the L_{VT} group, VT was 10 mL/kg, rat breathing

rates were 40 times/min, the ratio of inspiratoryexpiratory (I:E) was 1 to 2, positive end expiratory pressure (PEEP) was 0, fraction of inspired oxygen was 21% with 4 hours MV. In the H_{VT} group, VT was 35 mL/kg, the breathing rates of the rat were 50 times/min, the ratio of I:E was 1 to 2.5, p PEEP was 0, and the fraction of the inspired oxygen was 21% with 4 hours MV. A total of 5 mg/kg of RGDS peptide was added by means of an intra-abdominal injection 30 min before MV in the RGDS group with same MV parameter of the H_{VT} group. The model was established 4 hours after MV and pulmonary tissues collected on day 0, 3 and 7 were stored in –80 ℃.

Calculation of pulmonary index

On the 0, 3rd and 7th days post model establishment, five rats from each group were weighed and selected with both lung separation and pulmonary index calculated based on the following formula: pulmonary index = pulmonary weight (mg)/body weight (g).

Pulmonary hydroxyproline measurement

The rat lungs were collected on the 0, 3rd and 7th day after model establishment. The lungs were then grinded into powder in liquid nitrogen. The powder was re-constituted into homogenate (1 mL saline solution/per 100 mg powder) and then hydrolyzed in boiling water for 20 min. In order to measure the hydroxyproline concentration, a pH indicator was placed into the hydrolyzed homogenate before adjusting its PH to 6.0–6.8 according to the instruction of the HYDROXYPROLINE assay kit (Nanjing Jiancheng Bioengineering Institute, Nanjing, China). Next, they were added into 10 mL of distilled water, and acticarbon was put into the 3 mL of diluted hydrolysate with mixture and blending. Centrifugation at 3,500 rpm/min then took place and 1 mL of supernatant was selected for water bath at 60 ℃ for 10 min, cooled to room temperature and centrifuged again. The absorbance of the resultant supernatant was measured at 550 nm wavelength.

Determination of pulmonary alveolar inflammation and pulmonary fibrosis

On the 0, 3rd and 7th day after the rat model establishment, the selected left upper lung tissue slice of 2.0×2.0×0.3 cm^3 was washed with saline solution and the pulmonary tissues were made into paraffin sections. Hematoxylin-eosin (HE) and Masson staining were then performed to determine the pulmonary alveolar inflammation and pulmonary fibrosis respectively and histopathological changes were observed under the light microscope. Regarding the HE staining, the rat lung tissue was fixed in 4% paraformaldehyde for 48 hours and made into paraffin sections. The samples then underwent a process of dewaxing, haematoxylin staining for 5 min followed by dehydration with ethanol, sealing and drying with microscope observation. Pulmonary alveolar inflammation was divided into four grades on the basis of the Szapie *et al.* methods and judgement criteria were as follows: without alveolar catarrh (–); mild alveolar catarrh (1+) (widening of alveolar septum limited to part or near pleura with affected area <20% and normal alveolar structure); moderate alveolar catarrh (2+) (affected area between 20–50% more serious near pleura); severe alveolar catarrh (3+) [affected area >50% with occasional consolidation caused by monocytes and hemorrhage in alveolar space (AS)]. In regards to the Masson staining, the prepared sections were dewaxed and staining was then conducted using a Masson staining Kit (Nanjing Jiancheng Bioengineering Institute, Nanjing, China). More specifically, after staining with azure blue for 10 min and washing, the sections were then further stained with picric acid and sirius red for 30 min, washed with ethanol, dried and then sealed. The staining of collagen fibers was observed under a light microscope and the positive staining area was subsequently calculated. Pulmonary fibrosis was divided into 4 grades on the basis of the methods of Szapie *et al.*, and the judgment criteria were as follows: without fibrosis (–), mild fibrosis (1+) (affected area <20%), moderate fibrosis (2+) (affected area between 20–50%), severe fibrosis (3+) (affected area >50% with disordered alveolar structure). Both degrees of pulmonary alveolar inflammation and pulmonary fibrosis were assigned into four grades, denoted with 0, 1, 2, or 3 points from mild to severe depending on the respective situation. The histopathological changes were observed under a microscope, and the average of the five views that were randomly selected was calculated as the final point (17).

Reverse transcription quantitative polymerase chain reaction (RT-qPCR)

Rat lung tissues on the 0, 3rd and 7th day after model establishment were homogenized, and centrifuged at 3,000 rpm/min for 10 min at 4℃.The separated supernatant was aliquoted into 1.5 mL etoposide and cisplatin (EP) tubes. The aliquoted supernatants were then extracted

Table 1 The primer sequences for RT-qPCR

Primer	Sequence (5'-3')	Length (bp)
Wnt-5A	5'-GCACCAGAGCAGACAACCT-3'	101
	5'-GCCAGCATCACATCACAACA-5'	–
β-catenin	5'-GCTACTCAAGCTGATTTGATGGA-3'	120
	5'-GGTAGTGGCACCAGAATGGATT-3'	–
E-cadherin	5'-TTGCTACTGGAACAGGGACAC-3'	179
	5'-CCCGTGTTAGTTCTGCTGT-3'	–
Collagen I	5'-TCTGACTGGAAGAGTGGAGAGTA-3'	202
	5'-ATCCATCGGTCATGCTCTCG-3'	–
GAPDH	5'-GGATTTGGTCGTATTGGG-3'	205
	5'-GGAAGATGGTGATGGGATT-3'	–

GAPDH, glyceraldehyde-3-phosphate dehydrogenase; RT-qPCR, reverse transcription quantitative polymerase chain reaction

for RNA using an RNA extraction kit and the numbers were marked. RNA was extracted by polymerase chain reaction (PCR) kit, and then 2 μg of RNA was selected to synthesize the cDNA. After 3 μL of Oligo (dT) primer was added, diethyl phosphorocyanidated (DEPC) was added to the total volume of 13 μL with denaturation at 70℃ for 10 min. They were placed in ice immediately for 5 min, and 6 μL of 5× murine leukemia virus (MLV) buffer, 2 μL of deoxyribonucleoside triphosphates (dNTP), 0.5 μL of RNase inhibitor, 1.5 μL of moloney murine leukemia virus (MMLV) reverse transcriptase were added. The total volume was reached 30 μL by added DEPC. The cDNA was synthesized at 42 ℃ for 60 min, 95 ℃ 10 min and the reaction was then terminated. They were stored at –40 ℃ and reagents used in reversed transcription were purchased from Promega (Madison, WI, USA). RT-qPCR was employed to detect expressions of Wnt-5A, β-catenin, E-cadherin and collagen I, using glyceraldehyde-3-phosphate dehydrogenase (GAPDH) as the internal control. The primers were synthesized by Shanghai Sangon Biotech Co., Ltd., Shanghai, China (*Table 1*). RT-qPCR was conducted with a total volume of 20 μL, containing 10 μL of SYBR Green Master (Rox) (Roche, Basel, Swiss), 1 μL of each forward and reverse primer, 1 μL of cDNA and 7 μL DEPC. After mixing and centrifugation, RT-qPCR was performed with the following programs: pre-denaturation for 30 s at 95 ℃, 5 s at 95 ℃, 31 s at 60 ℃, 20 s at 95 ℃ and 60 s at 60 ℃ with 40 cycles. A solubility curve was constructed (60–90 ℃) to verify the specific amplification as the single product. The results were analyzed based on cycle threshold (Ct) value via relative quantity method compared with the internal reference GAPDH. The applied instrument was the real-time PCR (Eppendorf, Germany).

Western blotting

A total of 100 mg of rat lung tissues stored at –80℃ was selected, cut into pieces and placed into 1.5 mL EP tubes. Following the addition of 1 mL of animal tissue protein extraction reagent, the 100 mg of rat lung tissues were homogenized using supersonic homogenizer for 4–5 times until full pyrolysis, which was then stored in a fridge at 4 ℃ for 2 hours. The samples were then centrifuged at 10,000 g/min for 10 min in the cryogenic centrifuge. The supernatant of the cleared homogenate was aliquoted in the EP tubes and quantified for protein concentration detection by bicinchoninic acid (BCA) kit (Univ-bio, shanghai, China). In total, 40 μL of the extracted protein was applied for sodium dodecyl sulphate-polyacrylamide gel electrophoresis (SDS-PAGE) at 70 V for 120 min. They were then transferred into polyvinylidene fluoride (PVDF) membrane, blocked with 5% BAS for 1.5 hours. The membrane was incubated at 4 ℃ in a refrigerator overnight with the following primary antibodies: anti-Akt Mab (1:3,000), anti-p-Akt Mab (1:3,000), anti-α7Mab, anti-β1Mab (1:1,000) and anti-laminin (1:1,000), anti-GAPDH Mab (1:4,000) (purchased from Abcam, Cambridge, MA, USA). The membranes were then washed 3 times with tris-buffered saline tween 20 (TBST) (pH7.4), followed by incubation with rabbit-anti-mouse (IgG)-horseradish peroxidase (HRP) (1:2,000) for 1 hour at room temperature. Electrochemiluminescence (ECL) reagent was added to develop photos and the resultant photos were then scanned for protein level quantification using Image software. GAPDH served as the internal reference, and the formula was as follows: relative expression = scanning grey $level_{target\ protein}$/scanning grey $level_{internal\ reference}$. The experiments were repeated three times.

Immunohistochemistry staining

The rats were executed 4 hours after MV at 0, 3 and 7 days, and the left lower lobe pulmonary tissues were taken with paraffin embedding. They were then sliced and the slice thickness was approximately 4 μm. Rabbit-anti-mouse fibronectin (FN) (1:200) was purchased from GIBCO BRL (Grand Island, NY, USA) and Biotin-

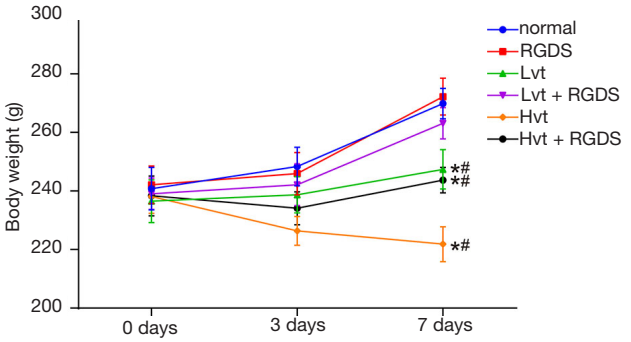

Figure 1 Rat weight changes in each group on 0, 3 and 7 days after MV. *, compared with the normal group, P<0.05; #, compared with the RGDS group, P<0.05; LVT, low tidal volume; HVT, huge VT; MV, mechanical ventilation; RGDS, Arg-Gly-Asp-Ser.

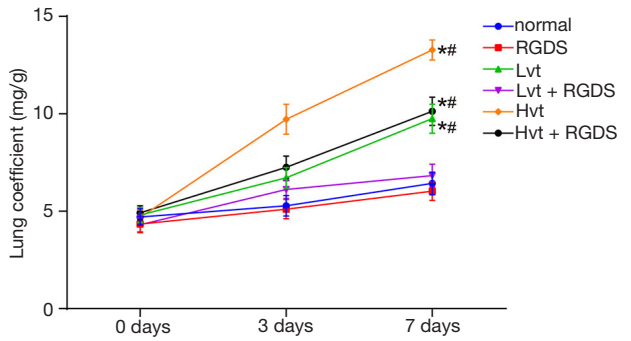

Figure 2 Pulmonary index changes in each group on 0, 3 and 7 days after MV. *, compared with the normal group, P<0.05; #, compared with the RGDS group, P<0.05; LVT, low tidal volume; HVT, huge VT; MV, mechanical ventilation; RGDS, Arg-Gly-Asp-Ser.

goat-anti-rabbit IgG and diaminobenzidine (DAB) were purchased from DAKO (Glostrup, Denmark). The slices were placed at room temperature for 60 min and then immerged into dimethylbenzene. Ethanol was applied to dewax and hydrate slices and then sealing fluid was added. The slices were then placed at room temperature for 20 min, and the primary antibody (Rabbit-anti-mouse FN, 50 μL) was put in for 1 hour at room temperature. Next, the secondary antibody (Biotin- goat-anti-rabbit IgG) was added, and DAB coloration was conducted after slices were washed out. Hematoxylin staining was used for 2 min, and the slices were then differentiated by hydrochloric acid and ethanol with dehydration, transparency, mounting and microscopy. Whether or not the expression was positive or not was determined by examining if the membranes had yellow granule. The positive staining area was calculated, and the score criteria of revised Hercep Test were applied to determine the positive expression: 0, 0< membrane coloration <10%; 1+, 10%< under or moderate standing of tumor cells <50%; 2+, 10%< strong standing of tumor cells <50%; 3+, staining of tumor cells (with arbitrary intensity) >50% (18,19).

Statistical analysis

Data were analyzed using SPSS21.0 statistics software (SPSS Inc., Chicago, IL, USA). The measurement data were represented as mean ± standard deviation (SD). *T*-tests were carried out for comparison between two groups while one-way analysis of variance (ANOVA) was used among multiple groups. P<0.05 indicated statistical significance.

Results

Results of rat weights in each group

As shown in *Figure 1*, the rat weights in the normal and RGDS groups kept gaining consistently between 0 and 7 days. Also, those in the L_{VT} and L_{VT} + RGDS groups displayed slight increases in weight. After 7 days, the weights of the two groups were lower than those in the normal group (P<0.05). Severn days later, compared with the L_{VT} group, the L_{VT} + RGDS group showed an up-regulation of weight (P>0.05), while the H_{VT} group presented down-regulated weight figures; lower than the normal group (P<0.05). Weights in the H_{VT} + RGDS group were higher than those in the H_{VT} group, but lower than those in the normal group (P<0.05).

Determination of rat pulmonary index in each group

Compared with the normal group, the pulmonary index in the L_{VT}, H_{VT}, L_{VT} + RGDS and H_{VT} + RGDS groups increased unanimously (P<0.05), with no difference in the RGDS group (P<0.05). On day 7, the H_{VT} group exhibited the highest pulmonary index figure, but the L_{VT} + RGDS group indicated a lower pulmonary index than the L_{VT} group (P<0.05), and higher than the normal group (P>0.05). On day 7, the pulmonary index in the H_{VT} + RGDS group was lower than that of the H_{VT} group, but higher than that in the normal group (all P<0.05, *Figure 2*).

Table 2 Measured hydroxyproline concentration in each group on 0, 3 and 7 days

Group	Day 0 (mg/g)	Day 3 (mg/g)	Day 7 (mg/g)
The normal group	0.99±0.11	1.10±0.03	1.11±0.06
The RGDS group	1.06±0.09	1.08±0.05	1.12±0.04
The L_{VT} group	1.05±0.07	1.13±0.11	1.29±0.12*
The L_{VT} + RGDS group	0.95±0.08	1.02±0.04	1.09±0.02
The H_{VT} group	1.18±0.12*	1.64±0.10*&	2.14±0.18*&
The H_{VT} + RGDS group	0.97±0.04#	1.36±0.10*#&	1.74±0.10*#&

*, compared with the normal group, P<0.05; #, compared with the HVT group, P<0.05; &, compared with the same group on day 0, P<0.05. L_{VT}, low tidal volume; H_{VT}, huge tidal volume; RGDS, Arg-Gly-Asp-Ser.

Pulmonary hydroxyproline in each group

As shown in *Table 2*, the hydroxyproline content (mg/g) remained unaltered in the normal and RGDS groups during the observation period. With the increase in days, when compared with the normal group, hydroxyproline in the L_{VT} and L_{VT} + RGDS groups increased slightly on day 3 with no statistical difference (P>0.05), however the L_{VT} group displayed significantly up-regulated levels on day 7 (P<0.05). On day 3 and 7, the H_{VT} and H_{VT} + RGDS groups showed higher hydroxyproline (P<0.05). In addition, the L_{VT} group had the higher hydroxyproline than the L_{VT} + RGDS group, but lower hydroxyproline than the H_{VT} group (all P<0.05). Hydroxyproline in the H_{VT} + RGDS group increased gradually over time and was higher than that in the normal group on 3 and 7 days (P<0.05). Compared with the H_{VT} group, the H_{VT} + RGDS group had lower hydroxyproline on 3 and 7 days (P<0.05).

Comparisons of pulmonary alveolar inflammation and pulmonary fibrosis in each group

Rat pulmonary tissues were collected and pathological changes of the alveolar structure were observed after HE staining on day 0, 3 and 7 after MV. As indicated in *Figure 3*, there were no morphology abnormalities observed in the lung tissues in the normal and RGDS groups; likewise, there was neither inflammatory cell infiltration nor essential collagen deposition under microscope observation over time. No apparent tissue morphology differences were detected between the L_{VT} and normal groups; however, some inflammatory cell infiltration in certain areas and alveolar septum enlargement were detected in the L_{VT} group. In addition, more cells that are inflammatory were exuded and broadened alveolar septum was more serious. Besides, the symptom of alveolar inflammation in the L_{VT} + RGDS groups decreased. Meanwhile, obvious inflammatory cell infiltration, septum enlargement, disruption of alveolar structure and alveoli congestion were observed in the H_{VT} group. As time went on, the situation became more and more serious. Compared with the H_{VT} group, the symptom of alveolar inflammation in the H_{VT} + RGDS groups was reduced on 3 and 7 days (all P<0.05). In addition, the pathological changes in each group were obviously aggravated and alveolar inflammation was increased except the normal and RGDS groups (all P<0.05).

As shown by the Masson stain in *Figure 4*, the extent of pulmonary fibrosis in the RGDS, L_{VT}, L_{VT} + RGDS groups was not significantly different from that in the normal group, however, in the H_{VT} group, some alveoli structures vanished while there were apparent increasing fibroblast and considerable fibroplasias, as substantial amount of collagen fiber was stained as blue. While less stained collagen fiber was observed in H_{VT} + RGDS group and fibrosis progression was delayed to some extent compared with the H_{VT} group. Besides, pulmonary fibrosis in the H_{VT} group was more serious than that in the L_{VT} group (P<0.05), and proliferation of fibrous tissues in each group becomes more and more serious.

The mRNA and protein expression of Wnt-5A, β-catenin, E-cadherin and collagen I in lung tissue

Compared to the normal group, mRNA and protein expressions of Wnt-5A, β-catenin, E-cadherin and Collagen I in the L_{VT}, RGDS and L_{VT} + RGDS groups remained unchanged, while significant increases in E-cadherin

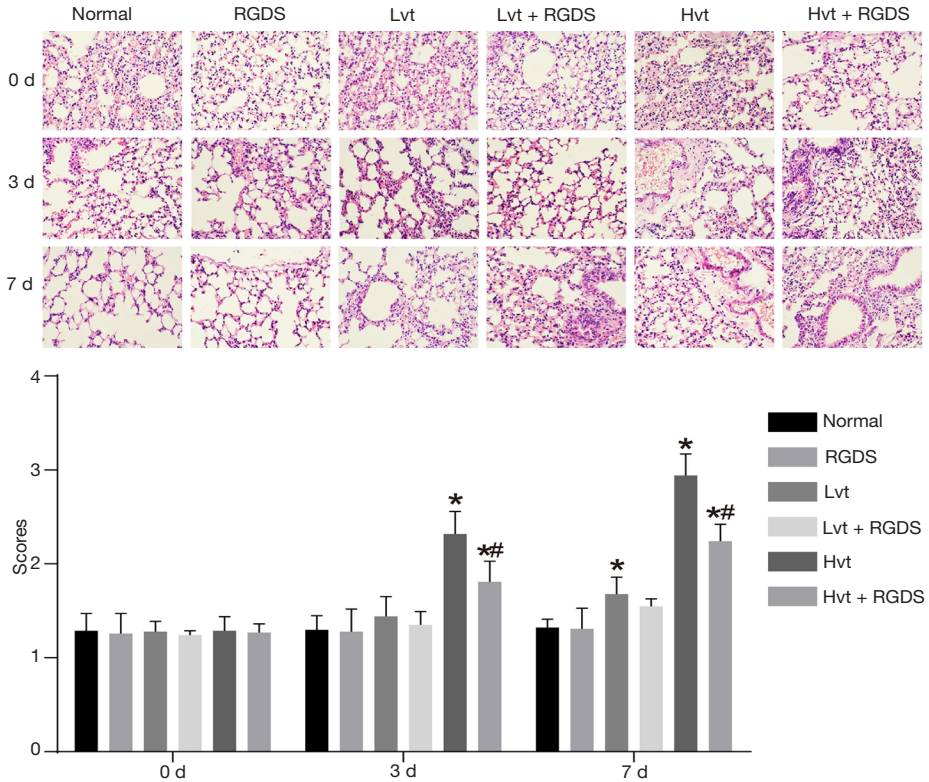

Figure 3 Histopathological scores of lung tissues in each group on 0, 3 and 7 days after MV using HE staining (×200). *, compared with the normal group, P<0.05; #, compared with the RGDS group, P<0.05; LVT, low tidal volume; HVT, huge VT; MV, mechanical ventilation; RGDS, Arg-Gly-Asp-Ser.

mRNA and protein expressions were decreased in the H_{VT} group with the exception of β-catenin (P<0.05, *Figure 5*). Compared to the L_{VT} group, the mRNA and protein expressions of Wnt-5A, β-catenin and Collagen I in the H_{VT} group were up-regulated as well as exhibiting down-regulated E-cadherin mRNA and protein expressions (P<0.05). Compared with the H_{VT} group, the mRNA and protein expressions of Wnt-5A, β-catenin and collagen I in the H_{VT} + RGDS group were all decreased though they were still higher than those in the normal group (P<0.05). Furthermore, the E-cadherin mRNA and protein expressions were increased but still lower than those in the normal group (P<0.05).

Lung tissue histochemistry observation

Immunohistochemistry results showed that on day 0, the normal group displayed a relatively small FN expression, the L_{VT} and L_{VT} + RGDS groups revealed slightly increased FN expression, while the H_{VT}, RGDS and H_{VT} + RGDS groups illustrated significantly up-regulated FN expressions. The H_{VT} + RGDS group had lower FN expression than the H_{VT} group. Moreover, the FN expression in the L_{VT} group was lower than that in the H_{VT} group, with increases rates observed in each group over time (*Figure 6*).

Discussion

MV belongs to a severe respiratory disease with complex mechanisms, the treatment of which is still not clear (1). A previous study demonstrated that Integrin α7β1 could bind with specific LN, while an *in vitro* study indicated that the activation of macrophages is mediated by integrin α7β1 (20,21). However, the mechanism of laminin-integrin α7β1 affecting MV-induced pulmonary fibrosis is yet to be reported on. Thus, this study was conducted accordingly with this in mind.

Pulmonary index is a critical indicator of pulmonary

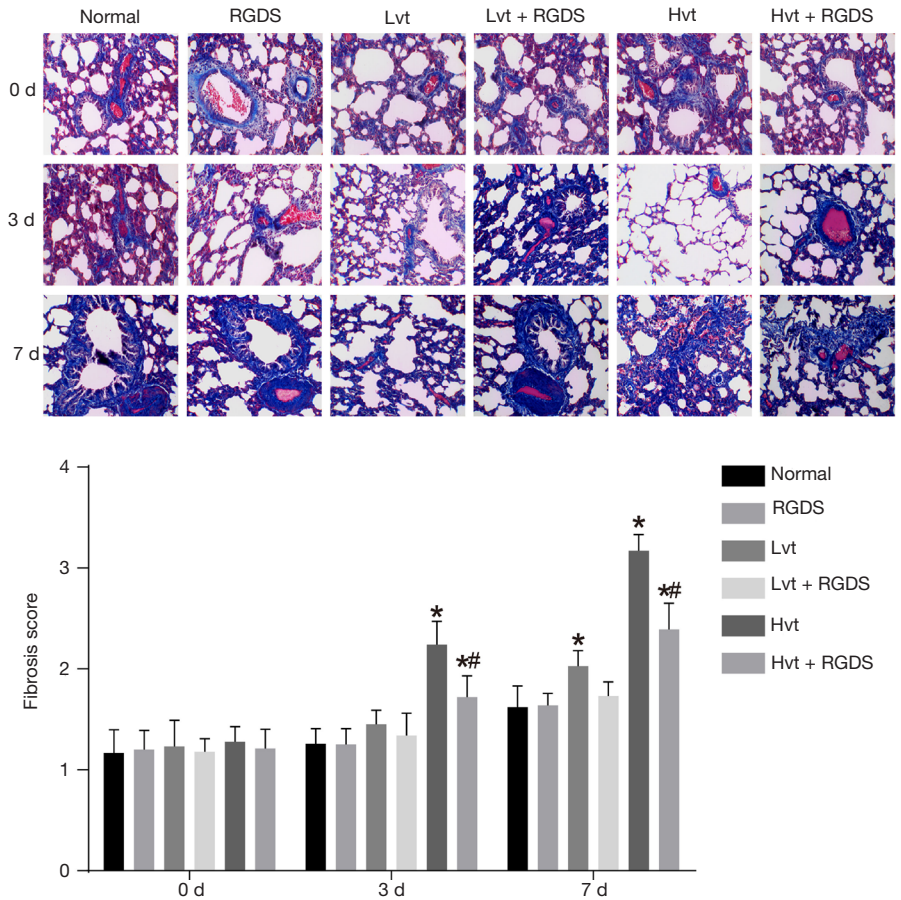

Figure 4 Masson staining density results in each group on 0, 3 and 7 days after MV (× 400). *, compared with the normal group, P<0.05; #, compared with the RGDS group, P<0.05; LVT, low tidal volume; HVT, huge VT; MV, mechanical ventilation; RGDS, Arg-Gly-Asp-Ser.

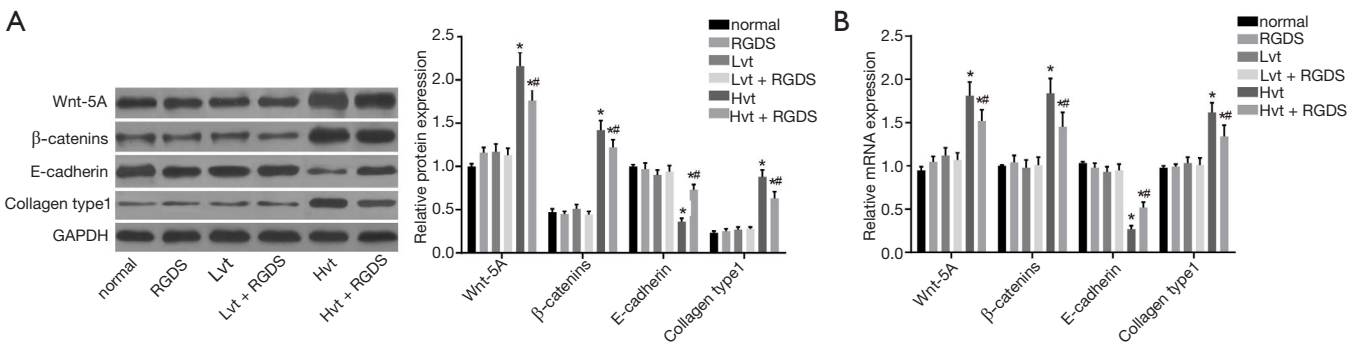

Figure 5 mRNA and protein expressions of Wnt-5A, β-catenin, E-cadherin and collagen I in each groups. *, compared with the normal group, P<0.05; #, compared with the RGDS group, P<0.05; LVT, low tidal volume; HVT, huge VT; RGDS, Arg-Gly-Asp-Ser; GAPDH, glyceraldehyde-3-phosphate dehydrogenase.

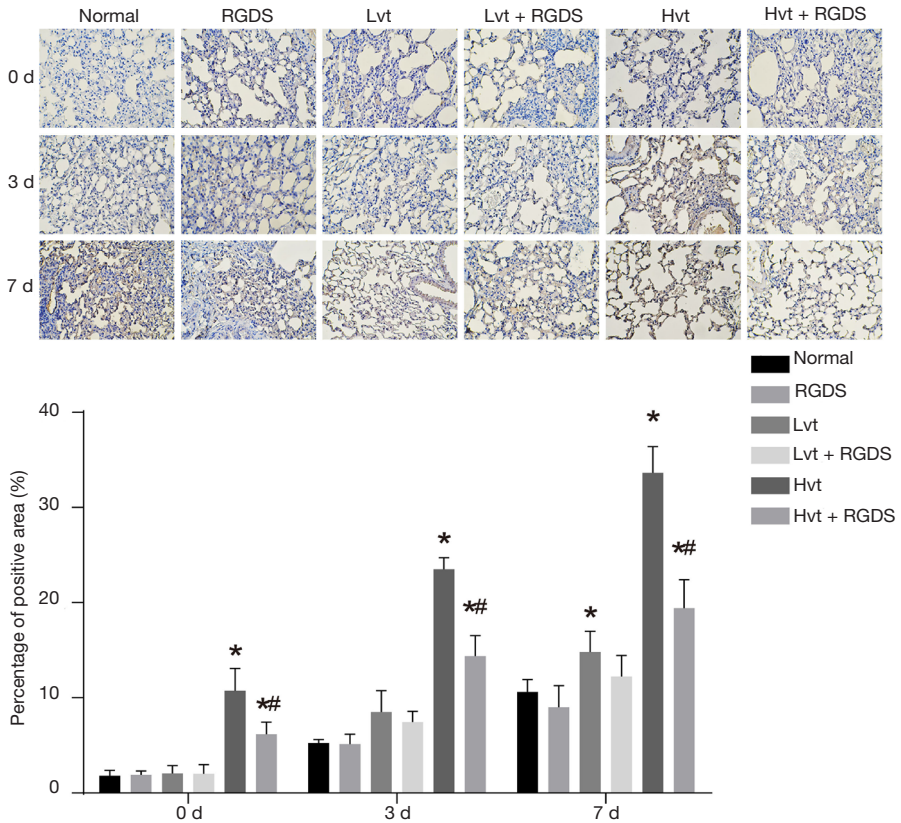

Figure 6 FN expressions in each group on 0, 3 and 7 days after MV using immunohistochemistry staining (× 200). *, compared with the normal group, P<0.05; #, compared with the RGDS group, P<0.05; LVT, low tidal volume; HVT, huge VT; MV, mechanical ventilation; RGDS, Arg-Gly-Asp-Ser; FN, fibronectin.

fibrosis. As fibrosis progresses, lung congestions and pulmonary cells begin to swell, which can lead to increases in lung weight, which subsequently increases lung indexes (22). As a collagen-specific constituent, hydroxyproline makes up to 13% of collagen, rendering it a perfect indicator of collagen presence as well as collagen deposition based on pulmonary fibrosis progression (23). Previous research revealed that various extents of lung tissue injury and structure alteration were observed after MV with different VTs, large VT in particular has resulted in dramatically increased septal inflammatory cell infiltration, alveolar wall thickening, alveolar structure destruction and even congestion (24). In this study, our data indicated that post RGDS peptide could be blocked in our rat model, the large VT induced pulmonary fibrosis symptoms/parameters (lung index, hydroxyproline level and pulmonary pathology evidence) were all mitigated and even reversed, suggesting that the blocked laminin-integrin α7β1 signaling pathway can inhibit pulmonary fibrosis.

To further elucidate the mechanism at work, our research revealed that in the process of MV-induced fibrosis, mRNA and protein expressions of Wnt-5A, β-catenin, collagen I and FN were up-regulated, while E-cadherin mRNA and protein level was down-regulated. Interruption of the laminin-integrin α7β1 signaling pathway apparently reversed the trends and inhibited the fibrosis progression. Thus, we ultimately postulated that blocking the laminin-integrin α7β1 signaling pathway exerts an alleviatory effect on MV-induced pulmonary fibrosis through the Wnt/β-catenin signaling pathway.

Wnt5a (Wingless-typefamilymember5A) is one of the well-studied Wnt families recently and it regulates cell responses through the canonical Wnt signaling pathway or non-canonical signal pathways (25). A previous study revealed the significance of Wnt5a expression in the FN cells of lung tissues, suggesting that Wnt5a plays

an important role in the development of idiopathic pulmonary fibrosis and some other fibroses interstitial lung diseases (6). β-catenin, a critical protein in the canonical Wnt pathway, controls cell response via regulating T-cell factor/lymphoid enhancer factor (TCF/LEF) gene transcription (26). Research from Lam *et al.* suggested that the hallmark of pulmonary fibrosis to be the accumulation of β-catenin in the cell nucleus of pulmonary fibroblasts and subsequent activation of its signal pathway (27). As an important member of the collagen family, Collagen I is extensively present around the bronchus, in the matrix surrounding blood vessels and alveolar septum. Some studies have provided evidence verifying that collagen I accumulates in concert with the progression of pulmonary fibrosis and measurements of collagen I accumulation foretells the disease progression of pulmonary fibrosis (28,29). There has been a general academia consensus in that FN is widely present non-collagen glycoprotein with numerous biological functions. Recent studies have observed considerably enhanced FN formation as well as upregulation of fibroblasts mitosis and proliferation in cases of pulmonary fibrosis (30). E-cadherin (CDH1) belongs to family of cadherin, which is a typical epithelial cell surface marker. In pulmonary fibrosis, E-cadherin expression is inversely correlated with β-catenin expression (31). Activation of this signaling pathway can trigger the fibroblast cell phenotype switch, stimulate pulmonary epithelial cells and promote the proliferation of medius fibroblast, inhibition of which can delay/mitigate the fibrosis of lung tissues (32). Some studies suggested that the activation of the Wnt signal pathway acts to promote pulmonary cell differentiation, while the Wnt/β-catenin signaling pathway is the crucial pathway of pulmonary fibrosis genesis and abnormal tissue repair and cell renewal Previous research has indicated the possibility to retard the cell phenotype switch and decrease chances of fibrosis through disruption of the target TCF/LEF family gene regulator (33,34). Therefore, interference of this signal pathway has much promise as a new therapeutic target for MV-induced pulmonary fibrosis (6,35).

Most importantly, our research presented convincing data and demonstrated that blocking the laminin-integrin signaling pathway up-regulates the expression of Wnt5a, β-catenin, collagen I and FN and down-regulates E-cadherin expression, through the Wntβ-catenin signaling pathway in the molecular level. This subsequently acts to suppress fibroblast proliferation in lung tissues and ultimately inhibits the fibrosis progression of lung.

Conclusions

Our study demonstrated that blocking the laminin-integrin α7β1 signaling pathway suppresses the progression of MV-induced pulmonary fibrosis through activating Wnt/β-catenin signaling pathway. We strongly feel that this discovery offers guidance and sheds lights on the clinical treatments of pulmonary fibrosis. Despite the detailed mechanism of inhibition on a molecular level still requires clarification. We anticipate that this discovery may lay a theoretical foundation for further study of the signal pathway of MV-induced pulmonary fibrosis ultimately offering a new perspective on the treatment of this disease.

Acknowledgements

We would like to acknowledge the helpful comments on this paper received from our reviewers.

Footnote

Conflicts of Interest: The authors have no conflicts of interest to declare.

Ethical Statement: The study was approved by the Animal ethics Association of the Shanghai 9th People's Hospital, Shanghai Jiao Tong University School of Medicine (Grant No. 201603001).

References

1. Hussain SN, Mofarrahi M, Sigala I, et al. Mechanical ventilation-induced diaphragm disuse in humans triggers autophagy. Am J Respir Crit Care Med 2010;182:1377-86.
2. Determann RM, Royakkers A, Wolthuis EK, et al. Ventilation with lower tidal volumes as compared with conventional tidal volumes for patients without acute lung injury: a preventive randomized controlled trial. Crit Care 2010;14:R1.
3. Cabrera-Benitez NE, Laffey JG, Parotto M, et al. Mechanical ventilation-associated lung fibrosis in acute respiratory distress syndrome: a significant contributor to poor outcome. Anesthesiology 2014;121:189-98.
4. Silva Santos P, Cruz C, Esquinas AM. Mechanical ventilation in idiopathic pulmonary fibrosis: Unresolved

dilemma. Respir Med 2016;117:283.
5. Strieter RM, Mehrad B. New mechanisms of pulmonary fibrosis. Chest 2009;136:1364-70.
6. Villar J, Cabrera NE, Valladares F, et al. Activation of the Wnt/beta-catenin signaling pathway by mechanical ventilation is associated with ventilator-induced pulmonary fibrosis in healthy lungs. PLoS One 2011;6:e23914.
7. Nelson J, McFerran NV, Pivato G, et al. The 67 kDa laminin receptor: structure, function and role in disease. Biosci Rep 2008;28:33-48.
8. Sannes PL, Wang J. Basement membranes and pulmonary development. Exp Lung Res 1997;23:101-8.
9. Durbeej M. Laminins. Cell Tissue Res 2010;339:259-68.
10. Singer, II, Kawka DW, McNally SM, et al. Extensive laminin and basement membrane accumulation occurs at the onset of bleomycin-induced rodent pulmonary fibrosis. Am J Pathol 1986;125:258-68.
11. Madamanchi A, Santoro SA, Zutter MM. alpha2beta1 Integrin. Adv Exp Med Biol 2014;819:41-60.
12. Lueders TN, Zou K, Huntsman HD, et al. The alpha7beta1-integrin accelerates fiber hypertrophy and myogenesis following a single bout of eccentric exercise. Am J Physiol Cell Physiol 2011;301:C938-46.
13. de Rezende FF, Martins Lima A, Niland S, et al. Integrin alpha7beta1 is a redox-regulated target of hydrogen peroxide in vascular smooth muscle cell adhesion. Free Radic Biol Med 2012;53:521-31.
14. Guo C, Willem M, Werner A, et al. Absence of alpha 7 integrin in dystrophin-deficient mice causes a myopathy similar to Duchenne muscular dystrophy. Hum Mol Genet 2006;15:989-98.
15. Boppart MD, Burkin DJ, Kaufman SJ. Activation of AKT signaling promotes cell growth and survival in alpha7beta1 integrin-mediated alleviation of muscular dystrophy. Biochim Biophys Acta 2011;1812:439-46.
16. Tran T, Ens-Blackie K, Rector ES, et al. Laminin-binding integrin alpha7 is required for contractile phenotype expression by human airway myocytes. Am J Respir Cell Mol Biol 2007;37:668-80.
17. Szapiel SV, Elson NA, Fulmer JD, et al. Bleomycin-induced interstitial pulmonary disease in the nude, athymic mouse. Am Rev Respir Dis 1979;120:893-9.
18. Kozu Y, Tsuta K, Kohno T, et al. The usefulness of mutation-specific antibodies in detecting epidermal growth factor receptor mutations and in predicting response to tyrosine kinase inhibitor therapy in lung adenocarcinoma. Lung Cancer 2011;73:45-50.
19. Yu J, Kane S, Wu J, et al. Mutation-specific antibodies for the detection of EGFR mutations in non-small-cell lung cancer. Clin Cancer Res 2009;15:3023-8.
20. von der Mark H, Williams I, Wendler O, et al. Alternative splice variants of alpha 7 beta 1 integrin selectively recognize different laminin isoforms. J Biol Chem 2002;277:6012-6.
21. Puklin-Faucher E, Gao M, Schulten K, et al. How the headpiece hinge angle is opened: New insights into the dynamics of integrin activation. J Cell Biol 2006;175:349-60.
22. Nalysnyk L, Cid-Ruzafa J, Rotella P, et al. Incidence and prevalence of idiopathic pulmonary fibrosis: review of the literature. Eur Respir Rev 2012;21:355-61.
23. Kleaveland KR, Velikoff M, Yang J, et al. Fibrocytes are not an essential source of type I collagen during lung fibrosis. J Immunol 2014;193:5229-39.
24. Saddy F, Sutherasan Y, Rocco PR, et al. Ventilator-associated lung injury during assisted mechanical ventilation. Semin Respir Crit Care Med 2014;35:409-17.
25. Logan CY, Nusse R. The Wnt signaling pathway in development and disease. Annu Rev Cell Dev Biol 2004;20:781-810.
26. Huang Z, Xie H, Ioannidis V, et al. Transcriptional regulation of CD4 gene expression by T cell factor-1/beta-catenin pathway. J Immunol 2006;176:4880-7.
27. Lam AP, Flozak AS, Russell S, et al. Nuclear beta-catenin is increased in systemic sclerosis pulmonary fibrosis and promotes lung fibroblast migration and proliferation. Am J Respir Cell Mol Biol 2011;45:915-22.
28. Moeller A, Gilpin SE, Ask K, et al. Circulating fibrocytes are an indicator of poor prognosis in idiopathic pulmonary fibrosis. Am J Respir Crit Care Med 2009;179:588-94.
29. Tsukui T, Ueha S, Abe J, et al. Qualitative rather than quantitative changes are hallmarks of fibroblasts in bleomycin-induced pulmonary fibrosis. Am J Pathol 2013;183:758-73.
30. Francois D, Venisse L, Marchal-Somme J, et al. Increased expression of protease nexin-1 in fibroblasts during idiopathic pulmonary fibrosis regulates thrombin activity and fibronectin expression. Lab Invest 2014;94:1237-46.
31. Lau MT, Klausen C, Leung PC. E-cadherin inhibits tumor cell growth by suppressing PI3K/Akt signaling via beta-catenin-Egr1-mediated PTEN expression. Oncogene 2011;30:2753-66.
32. Lam AP, Herazo-Maya JD, Sennello JA, et al. Wnt coreceptor Lrp5 is a driver of idiopathic pulmonary

fibrosis. Am J Respir Crit Care Med 2014;190:185-95.
33. Kim TH, Kim SH, Seo JY, et al. Blockade of the Wnt/beta-catenin pathway attenuates bleomycin-induced pulmonary fibrosis. Tohoku J Exp Med 2011;223:45-54.
34. Wang X, Dai W, Wang Y, et al. Blocking the Wnt/beta-Catenin Pathway by Lentivirus-Mediated Short Hairpin RNA Targeting beta-Catenin Gene Suppresses Silica-Induced Lung Fibrosis in Mice. Int J Environ Res Public Health 2015;12:10739-54.
35. Wang C, Zhu H, Sun Z, et al. Inhibition of Wnt/beta-catenin signaling promotes epithelial differentiation of mesenchymal stem cells and repairs bleomycin-induced lung injury. Am J Physiol Cell Physiol 2014;307:C234-44.

Cite this article as: Liao HD, Mao Y, Ying YG. The involvement of the laminin-integrin α7β1 signaling pathway in mechanical ventilation-induced pulmonary fibrosis. J Thorac Dis 2017;9(10):3961-3972. doi:10.21037/jtd.2017.09.60